Medical University "Prof. Dr. Paraskev Stoyanov" – Varna
Faculty of Dental Medicine
Department of Periodontology and Dental Implantology

Dr. Konstantin Stoychev Kostadinov

Multimodal Imaging Documentation in Dental Medicine

ABSTRACT

of the dissertation for the award of the educational and scientific degree "DOCTOR"

SCIENTIFIC SPECIALTY:

Therapeutic Dentistry

ACADEMIC ADVISOR:

Prof. Dr. Stefan Vassilev Peev, DMD, PhD, DSc

Varna, 2023

The dissertation comprises 156 standard pages and is illustrated with 39 tables, 98 figures, 6 graphs, and includes 4 appendices. It cites 259 literary sources, 16 in Cyrillic and 243 in Latin script. The numbering of the tables and figures in the abstract does not correspond to those in the dissertation.

The dissertation has been approved for public defense by the departmental council of the Department of Periodontology and Dental Implantology on 21st September 2023.

The official defense of the dissertation will take place on 18th January 2023 in Auditorium 103 "Assoc. Prof. Dr. Dimitar Klisarov" at the Faculty of Dental Medicine, Medical University "Prof. Dr. Paraskev Stoyanov" – Varna, during a session of the scientific jury.

The materials for the defense are available at the Scientific Department of MU-Varna and have been published on the MU-Varna website.

Content

Abbreviations used

CBCT – Cone Beam Computed Tomography

CMM – Coordinate Measuring Machine

DICOM – Digital Imaging and Communication in Medicine

FOV – Field of View HSDM -

Harvard School of Dental Medicine

ICC – Intraclass Correlation Coefficient

IOS – Intraoral Scanner

MDCT – Multidetector Computed Tomography

PCIN – Polymer Infiltrated Ceramic Network

ROI – Region of Interest

STL – Stereolithography

3D – Three-Dimensional

1. INTRODUCTION

Dental Medicine is a branch of medicine that involves the study, diagnosis, prevention, and treatment of diseases, disorders, and conditions of the oral cavity, most commonly the teeth (including their development and arrangement), as well as the oral mucosa, and adjacent and related structures and tissues, especially in the maxillofacial (jaw and facial) area.

The history of dentistry is nearly as ancient as the history of humanity and civilization, with the earliest evidence dating back to 7000 to 5500 BCE. It is considered that dentistry is the first specialty in medicine that developed its own accredited degree with specialized fields. The modern evidence-based dentistry movement advocates the use of high-quality scientific research and evidence to guide decision-making in managing oral diseases.

Dental medicine is evolving at exceptionally rapid rates, and one of the main reasons for this is the integration of digital technologies into its various fields. Examples of this include intraoral scanners (as an alternative to conventional impression techniques and materials), digital sensors (as an alternative to analog dental films), and the increasingly widespread use of Cone Beam Computed Tomography (CBCT) scanners for the everyday needs of dental practice.

In daily practice, conventional methods, materials, and techniques that have proven to be reliable means of dealing with various clinical problems are still widely used. Various procedures are based on intraoral impressions, including therapeutic planning, diagnosis, patient communication, making casts, and producing prosthetic restorations and appliances for various applications. Over the years, new materials have emerged or existing ones have been improved upon. A clear example is impression-taking materials, which are still widely used and have undergone numerous changes and enhancements. Using these impressions, we can obtain plaster models that replicate the patient's clinical situation. These models serve for more precise planning and execution of the treatment plan, and also serve as a fundamental means of communication between dental practitioners and dental laboratories.

Due to technological progress, various intraoral scanners have become increasingly common in the market, allowing us to obtain digital models as an alternative to conventional methods. Working with intraoral scanners offers several advantages:

- Good tolerance, even in patients with a gag reflex.
- Ability to re-scan specific areas of the prosthetic field.
- Relatively fast execution.
- No risk of transmitting infections to the dental laboratory.
- Improved communication with the dental laboratory.
- Easy storage of the digital model.

A relative drawback remains the high cost of purchasing such scanners.

The accuracy of various impression-taking materials and modalities has been widely debated by different authors, and to this day, there is no unanimous consensus on whether conventional or digital techniques are more accurate. The precision of the model is of utmost importance in certain areas of dental medicine, where deviations over 200 microns are clinically significant, as in implantology, where integrated implants are firmly anchored in the alveolar bone, and inaccuracies in the implant impression can compromise the fit of the implant prosthesis, potentially leading to biological and mechanical complications. In orthodontics and prosthetic restorations on natural teeth, larger deviations are permissible due to the natural mobility of the teeth.

Most studies on the accuracy of different impression-taking methods are in vitro-based under optimal working conditions, reducing the likelihood of errors and deviations. There are no complicating factors such as patients' saliva, the presence of the tongue and cheeks, no collaboration issues, nor problems related to patients' gag reflex or vomiting during the experiments. In these test experiments, when evaluating various conventional impression materials, it's easy to extend the setting time of the material. Moreover, the shape of experimental models is often a regular geometric figure, which is far from the shape of natural teeth. All these factors can positively influence the end result, regardless of the method used for impression-taking in the prosthetic field.

The accuracy of the models can be measured through:

- Comparing linear measurements between a reference model/jaw and the same measurements on the obtained digital or analog model;
- By the accuracy of the fit of a prosthetic structure on a prepared tooth or on implants;

- Using best-fitting software.

There is a shortage of in-vivo studies, as it is challenging to create ideal and easily reproducible conditions for conducting experiments and measurements.

Digital technologies significantly influence the field of dental imaging diagnostics. With the introduction of Cone Beam Computed Tomography (CBCT), the possibilities for diagnosis, planning, and treatment have expanded across all areas of dental medicine. This modality overcomes the limitations associated with conventional imaging studies, such as two-dimensionality (superimposition of anatomical structures) and image distortion. The primary advantage of CBCT studies lies in the ability to observe the area of interest in three planes – axial, coronal (frontal), and sagittal – without superimposition of anatomical objects, as the position of the section observed can be manipulated for each plane. This allows a more accurate assessment of the analyzed area. The main factor that can deteriorate the quality of CBCT images is artifacts (distortion or errors in the image unrelated to the studied object). The formation of artifacts can be due to various reasons, with one of the most common being the so-called "motion artifacts," as well as artifacts resulting from the "beam hardening" phenomenon. One of the main limitations of this type of imaging remains the low contrast resolution, leading to lower soft tissue contrast in CBCT compared to Multidetector Computed Tomography (MDCT).

Using volume rendering/visualization software, 3D models (surface models) can be constructed from imported sets of Cone Beam Computed Tomography (CBCT) data by applying algorithms that are typically unique to each program. These 3D reconstructions, known as 3D Volume Rendering, allow actions such as marking landmarks, performing measurements, relocating bone fragments, and conducting virtual osteotomies. Therefore, the accuracy of the resulting model is of utmost importance not only for diagnostic purposes but also for treatment planning and its outcomes.

3D visualization enhances diagnosis and communication with patients and finds applications in various fields of dental medicine. Despite the advantages of this modality, it is not yet widely adopted in daily practice. One reason for this is the additional costs associated with purchasing and maintaining software for processing and analyzing 3D data, as well as the need for additional training and experience. The application of these types of 3D-generated models is still a subject of discussion and research. While literature provides data on their accuracy under various experimental conditions, there is a lack of studies that generalize their real-world application in clinical settings.

2. OBJECTIVES AND TASKS

Objective:

To investigate and compare the accuracy of tooth reconstruction based on generated 3D models from Cone Beam Computed Tomography (CBCT) and intraoral scanning, as well as on gypsum models from conventional impression materials, in comparison to the results of intraoral measurements with a digital caliper.

Tasks:

1. **Task:** Determine the accuracy of tooth reconstruction by generating a 3D model from CBCT data.
2. **Task:** Determine the accuracy of tooth reconstruction by generating a 3D model from an intraoral scanner.
3. **Task:** Determine the accuracy of tooth reconstruction by pouring gypsum models using polyether Impregum Monophase (3M ESPE) and A-silicone Elite HD+ (Zhermack).
4. **Task:** Establish the reliability and accuracy of each investigated method for reconstructing a diagnostic model of the lower jaw through the analysis of repeated linear measurements of interdental distances in the lower jaw.

3. OWN RESEARCH

3.1 MATERIALS

3.1.1. The study was conducted at:

- Faculty of Dental Medicine, Medical University of Varna

3.1.2. Object of Study

The study involved a total of 38 individuals (16 males and 22 females) with an average age of 29.8 years (ranging from 18 to 75 years), patients of the Faculty of Dental Medicine, Medical University of Varna. Forty individuals volunteered to participate, two of whom were excluded due to having prosthetic restorations (crowns) on more than one of the teeth necessary for the measurements in the lower jaw.

3.1.3. Patient Selection

The study included male and female patients over 18 years of age, in good general health, who required dental treatment involving CBCT as part of the diagnostic process. Each patient was informed about the purpose of the study and signed a declaration of informed consent (Appendix 2) for the necessary procedures and manipulations in this study, as well as a declaration for the X-ray examination (Appendix 4). Age, gender, and socio-economic status were not the primary factors in selecting participants for the study.

Inclusion Criteria: • Signed informed consent.

• Participants aged 18 and above.

• Gender: not a determining factor.

• Individuals without active orthodontic treatment.

• Individuals with up to one missing tooth in the first molar position.

• Individuals with up to one prosthetic restoration (crown) on the first molars on natural teeth.

• Individuals with first premolars and central incisors in the lower jaw.

• Good oral hygiene.

• Individuals in good general health.

Exclusion Criteria:

• Individuals with severe systemic diseases.

• Pregnancy and breastfeeding.

• Age under 18 years.

• Mental illnesses.

• Individuals with missing first premolars and central incisors in the lower jaw.

• Individuals with prosthetic restorations (crowns) on the first premolars and central incisors on natural teeth.

• Individuals with restorations on implants in the lower jaw.

• Acute and chronic inflammatory processes involving the hard and soft tissues in the oral cavity within the examination area.

• Individuals with advanced periodontitis.

• Individuals currently undergoing radiation therapy or chemotherapy.

For the purposes of the doctoral thesis, no surgical or other invasive procedures are planned, eliminating any health risks for the participants.

3.2 METHODS, RESULTS AND ANALYSES

Statistical methods

The results were recorded and processed using the following software:

• IBM SPSS Statistics

• Online Effect Size Calculator (Statistics Kingdom)

• G*Power.

The following statistical methods were applied for the statistical analysis of the research parameters:

• Descriptive statistics

• Hypothesis testing for the difference between means of two related samples (Paired t-test)/ Wilcoxon test

• Repeated measures ANOVA

• Pearson/Spearman correlation coefficient

• Kolmogorov-Smirnov test for normality of distribution

• Graphical and tabular methods for representing the obtained results

• Selected significance level α = 0.05

• Effect size (Cohen's D) with reference values for effect strength: for D from 0 to 0.3, the effect is considered small; for D from 0.3 to 0.7, the effect is considered moderate; and for D from 0.7 to 1, the effect is considered large.

• Minimum required sample size, with a significance level of α=0.05, power of the test 1-β=0.8, and considering a "moderate" effect size e n = 34:

• Minimum required sample size, with a significance level of α=0.05, power of the test 1-β=0.8, and considering a "large" effect size e n = 15:

The clinical study was conducted after obtaining approval from the Ethics Commission for Scientific Research at the Medical University of Varna - protocol/decision No. 131, session on May 11, 2023. All participants in the study have signed informed consent forms.

Methods for task 1

1. Placement of composite markers.
2. Physical measurements.
3. Scanning with cone-beam computed tomography.
4. Conversion from .dicom to .stl files from CBCT scans.
5. Conducting measurements on the digital models from CBCT.

PLACEMENT OF COMPOSITE MARKERS

Before conducting intraoral measurements with a digital caliper, composite markers/buttons were placed on the buccal surfaces of teeth 36, 46, 34, and 44 (Fig. 1) to serve as reference points for individual measurements. We used a two-step Etch&Rinse protocol. The buccal surface of the specified teeth was selectively etched around the equator for 20 seconds, then rinsed with water for a minimum of 10 seconds, and air-dried until a chalky white surface was visible, simultaneously using aspiration to remove excess moisture. Next, a one-component adhesive, Adhesive Universal Viva Pen, was applied for 10 seconds, followed by drying for another 10 seconds and light-curing with a photopolymerization lamp (3M Elipar Deep Cure, 3M ESPE) for 20 seconds. The composite buttons were created using a dual-cure composite material, Grandio Core Dual Cure (VOCO GmbH), which was mixed and applied using a self-mixing cannula immediately after curing the adhesive. The composite was light-cured for 40 seconds after application. We repeated the procedure for creating composite buttons for each tooth individually, aiming to maintain a dry working field using aspiration and cotton rolls in the area of the treated teeth to achieve the best bond between the composite and the tooth surfaces.

Fig. 1. Composite buttons on the buccal surfaces of teeth 36, 46, 34, 44.

PHYSICAL MEASUREMENTS

After creating the composite buttons, we conducted direct physical measurements intraorally using a digital caliper, Kinex (Kinex measuring, Czech Republic) (Fig. 2), with a range of 0-300 mm, jaw length of 60 mm, and a resolution of 0.01 mm. We measured the linear distances on the lower jaw between teeth 36-46, 34-44, 36-34, 46-44, 34 - midline between 31 and 41, 44 - midline between 31 and 41, always in this sequence (illustrated in Fig. 83 in "Measurements on Gypsum Models"). We used these values as control/reference values for comparison with other investigated modalities. The measurements were recorded in millimeters with a tenth of a millimeter accuracy. The composite buttons served as a reference point during the measurements – we placed the caliper jaws over the buttons as close to them as possible when measuring the distances between teeth 36-46, 34-44, 36-34, 46-44. When measuring the distances between 34 - midline between 31 and 41 and 44 - midline between 31 and 41, we placed one end of the caliper on a point between the central incisors in the middle 1/3 of the respective teeth. Before each new measurement, we zeroed and calibrated the caliper to reduce the likelihood of errors during the measurements. We recorded the measurement values in a table in Word (Microsoft) format (Appendix 1), which we later transferred to Excel 2019 (Microsoft).

Fig. 2. Digital Caliper Kinex (Kinex Measuring, Czech Republic)

SCANNING WITH CONE-BEAM COMPUTED TOMOGRAPHY

We conducted 3D imaging studies on each of the volunteers in the research using a cone-beam computed tomography (CBCT) machine for both the upper and lower jaws. We utilized the New Tom Giano HR Professional apparatus (2019) (Fig. 3) with the following parameters: tube voltage 90V, current 4mA, exposure time 8s, and a CMOS detector - a flat panel made of amorphous silicon transforming X-ray energy into digital signals. Isometric voxels with a size of 0.15mm (150 microns) were used for image reconstruction.

Fig. 3. Cone-Beam Computed Tomography Scanner New Tom Giano HR

Prior to the cone-beam computed tomography (CBCT) scanning, we obtained informed consent from each volunteer (Appendix 4) for the imaging study. Each participant in the study required dental treatment, which necessitated a scan that also included the upper jaw.

Before the scanning process, all metal objects within the examination area were removed, and a protective lead apron with a 0.50 mm lead equivalent was placed. During the examination, participants were in an upright position with the chin resting on a special support, the head stabilized in an immobile position, and the jaws fixed using a plastic plate that was bitten down on throughout the scanning process (Fig. 4).

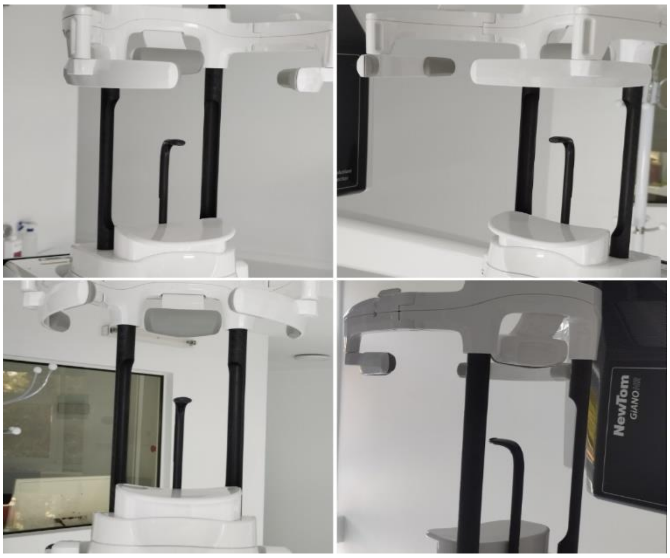

Fig. 4. Chin Rest, Head Support, and Bite Block on the Cone-Beam Computed Tomography Scanner.

We preset the scanning volume to 10x10 in the software. During the scanning process, the X-ray tube and detector rotated 360 degrees around the patient's head. Using an HP Z240 Tower Workstation with an Intel(R) Xeon(R) CPU E3-1270 v5, 3.60GHz processor, 8.00GB RAM, Windows 10 Pro, and NNT Viewer software, the acquired images were reconstructed in Multi-Planar Reconstruction (MPR) mode in three planes:

- Axial: separating the upper and lower parts of the object
- Sagittal: separating the left and right parts of the object
- Coronal: separating the front and back parts of the object

This study allowed for a comprehensive analysis of the dental and jaw apparatus. However, for the purposes of this dissertation, the focus was solely on the image of the lower jaw, with particular attention to the absence of motion artifacts that could compromise or even render the image unusable in subsequent stages of the study.

The obtained .DICOM files from the conducted 3D imaging studies were imported into Inversalius 3.1 software, which generated 3D models of the lower jaw in .STL file format. Linear measurements were then performed on these models using appropriate software tools, such as 3D Viewer (3Shape).

CONVERTING .DICOM TO .STL FILES FROM CBCT SCANS

We converted the generated DICOM files from the CBCT scans to STL files for the purpose of conducting linear measurements using suitable software. The conversion was performed using InVesalius 3.1 software.

The conversion process proceeded as follows: upon launching the software, we selected the option to import a file and chose the DICOM file from the conducted CBCT scans. During import, the percentage of the original resolution was set to 100. After the import process, we manually set a threshold value for tissue visualization. The chosen value for all files ranged from 1600 to 7500 (Fig. 5), allowing for the reduction of artifacts in the resulting 3D model and enhancing the visualization of the composite markers, which served as the primary reference points for conducting linear measurements.

Next, the unnecessary part of the file volume was cropped. This was done by selecting Tools → Mask → Crop from the dropdown menu. This cropping method expedited the conversion process and reduced the size of the resulting STL file. The cropping was carried out through subjective assessment, utilizing axial, sagittal, and coronal planes simultaneously (Figs. 6-8).

Subsequently, the command "Create surface" was given with the following parameters: Method: Context aware smoothing, Angle: 0.7, Max. distance – 1.20, Min. weight – 0.5, N.steps – 10 (Fig. 9). The resulting digital model (Fig. 10) was then exported and saved as an STL file in a folder titled "Dicom to STL".

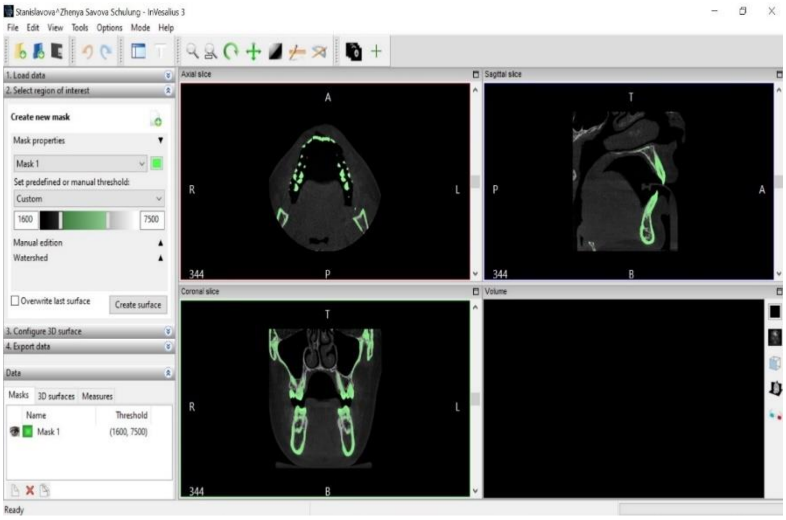

Fig. 5. Manual Setting of Threshold Values (1600-7500) for Tissue Visualization with Specific Density.

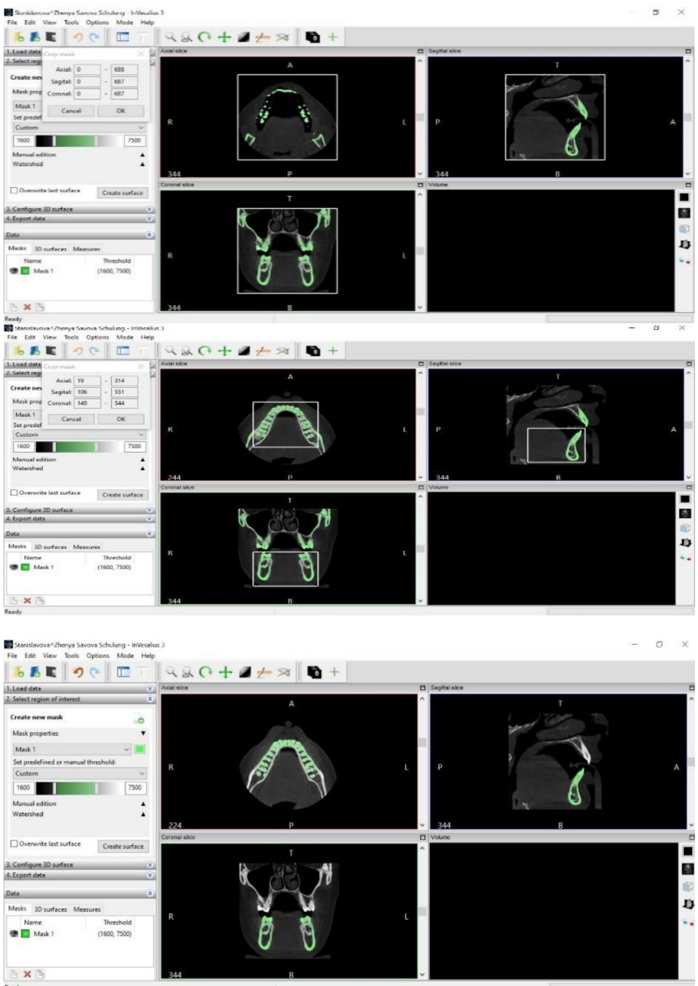

Fig. 6-8. Manual Cropping Process Based on Subjective Assessment for the Specific Patient.

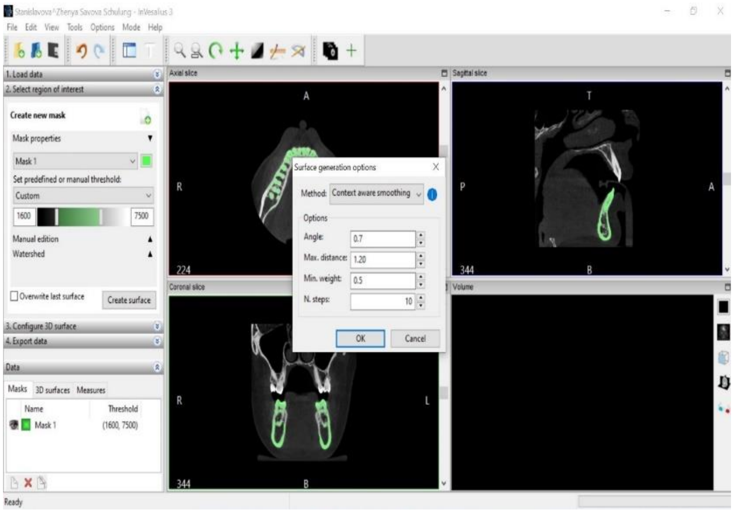

Fig. 9. Setting Parameters for "Create Surface".

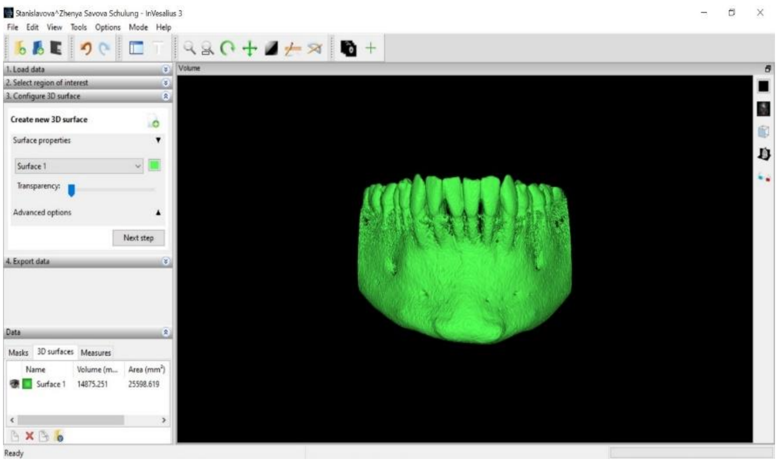

Fig. 10. The Generated 3D Model after Converting .dicom File to .stl File.

CONDUCTING MEASUREMENTS ON DIGITAL MODELS FROM CBCT SCANS

For conducting measurements on the 3D models derived from CBCT scans, we used the 3DViewer software (3Shape). After launching the software, an empty window is opened, from which we select the "File→Open" option. Then, we choose a file from the "Dicom to STL" folder and open it to perform the necessary measurements. As the software allows simultaneous measurement of up to three linear distances, the following approach was developed to optimize and achieve maximum accuracy in measuring the distances between teeth 36-46, 34-44, 36-34, 46-44, 34 - midline between 31 and 41, 44 - midline between 31 and 41:

1. Placing a digital marker on the midline between 31 and 41 (Figure 11).

2. Placing a digital marker above the composite marker on the buccal surface of 34 (Figure 12).
3. Placing a digital marker above the composite marker on the buccal surface of 36 and placing a second one on the first marker on the buccal surface of 34, aiming for maximum alignment between the markers (Figure 12).
4. Placing a digital marker above the composite marker on the buccal surface of tooth 44 and placing a second one on the buccal surface marker of tooth 34, aiming for maximum alignment (Figure 13).
5. Moving the first marker from the buccal surface of tooth 34 onto the marker on the buccal surface of tooth 44 (Figure 14).
6. Moving the second marker from the buccal surface of tooth 34 onto the buccal surface of tooth 46 above the composite marker (Figure 15).
7. Moving a marker from the midline between 31 and 41 onto the marker on the buccal surface of tooth 46 while ensuring a perfect fit between the markers (Figure 16).

In this way, the linear distances are measured in the following order:

1. 34 - midline between 31 and 41.
2. 34-36.
3. 34-44.
4. 44 - midline between 31 and 41.
5. 36-46.
6. 44-46.

For each 3D model, measurements are performed in this sequence to reduce the possibility of placing the markers in different positions each time. All measurements were conducted on a computer with the following specifications: Processor Intel(R) Core(TM) i7-9700F CPU @ 3.00GHz 3.00 GHz; RAM 16.0 GB, 64-bit operating system running Windows 10 Pro. The workstation is equipped with two 18-inch monitors (Figure 18).

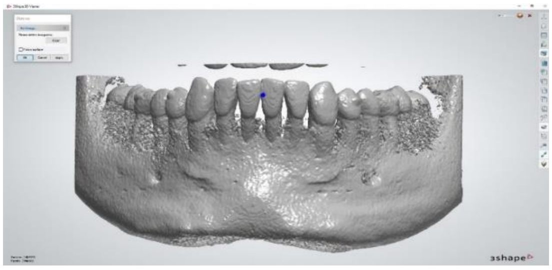

Fig. 11

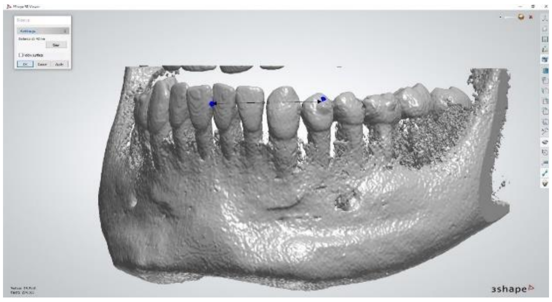

Fig. 12

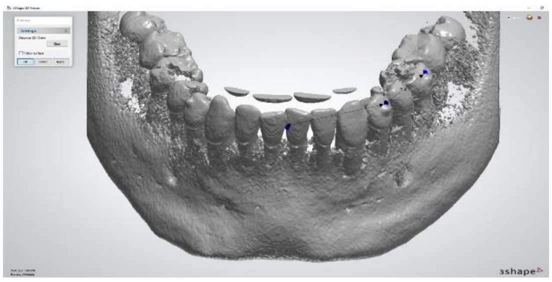

Fig. 13

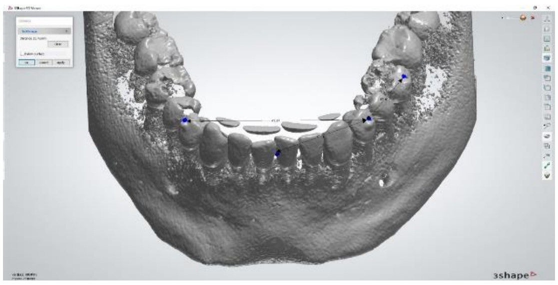

Fig. 14

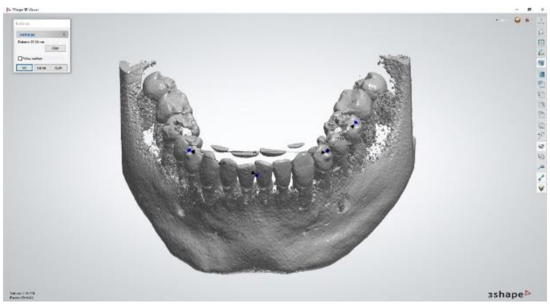

Fig. 15

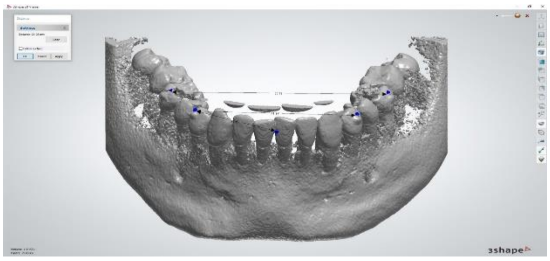

Fig. 16

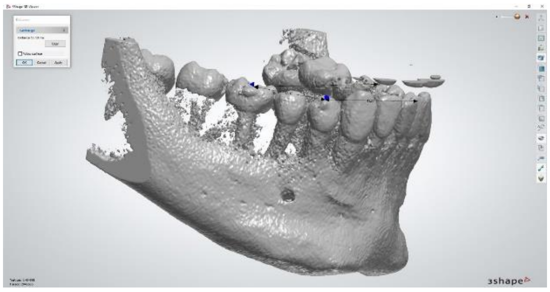

Fig. 17

Fig. 18. Workstation for Conducting Measurements on Digital Models.

Results for task 1

Table 1 presents descriptive characteristics of the results obtained from measurements on the 3D reconstruction generated from CBCT.

Table 1

Linear measurments	Modalities	N	Mean	SD	SE	CI 95% for Mean		Min	Max
						Low	Up		
46x36, mm	Physical measurments	36	48.893	3.33	0.56	47.77	50.02	41.06	56.60
	CBCT	33	49.015	3.37	0.59	47.82	50.21	41.62	56.50
44x34, mm	Physical measurments	38	36.59	2.80	0.45	35.67	37.51	30.53	41.53
	CBCT	38	36.44	2.79	0.45	35.52	37.36	30.21	41.53
36x34, mm	Physical measurments	37	15.84	1.07	0.18	15.49	16.20	13.70	18.20
	CBCT	36	16.11	1.06	0.18	15.76	16.47	13.97	18.15
46x44, mm	Physical measurments	36	15.41	2.29	0.38	14.63	16.18	8.47	20.39
	CBCT	34	15.61	2.51	0.43	14.74	16.49	8.24	20.91
34x31/41, mm	Physical measurments	38	20.49	1.53	0.25	19.99	20.99	16.84	23.62
	CBCT	38	20.70	1.56	0.25	20.18	21.21	17.60	24.79
44x31/41, mm	Physical measurments	38	20.69	1.57	0.26	20.17	21.21	17.35	24.16
	CBCT	38	21.13	1.58	0.26	20.61	21.65	17.97	24.52

Analysis for task 1

Comparing the results of linear measurements of interdental distances in the lower jaw between direct intraoral measurements with a digital caliper and those made on generated 3D diagnostic models from the CBCT scanner led to the following observations:

Control_46x36 & 3D_CBCT_46x36

Table 2

P-value	0.09469
T	-1.7222
Sample size(n)	33
Average of differenceces ($\overline{x_d}$)	-0.1285
SD of differences (S_d)	0.4286

From the above data, with the established p-value (0.09) > α => H0 cannot be rejected. This means that the mean value for the general population for 3D_CBCT_46x36 can be assumed to be equal to the mean value for the general population for Control_46x36. Effect size: d = 0.30 => small effect size, indicating that the difference between the mean values of the differences and the expected mean value of the differences is small.

Control_44x34 & 3D_CBCT_44x34

Table 3

P-value	0.03297
T	2.2153
Sample size(n)	38
Average of differenceces ($\overline{x_d}$)	0.1461
SD of differences (S_d)	0.4064

From the above data, with the established p-value (0.03) < α => H0 is rejected in favor of H1. This means that the mean value for the general population for 3D_CBCT_44x34 can be assumed to be different from the mean value for the general population for Control_44x34, or the difference is statistically significant. Effect size: d = 0.36 => small effect size, indicating that the difference between the mean values of the differences and the expected mean value of the differences is small.

Control_36x34 & 3D_CBCT_36x34

Table 4

P-value	0.0009527
T	-3.6084
Sample size(n)	36
Average of differenceces ($\overline{x_d}$)	-0.2711
SD of differences (S_d)	0.4508

From the above data, with the established p-value (0.00) < α => H0 is rejected in favor of H1. This means that the mean value for the general population for 3D_CBCT_36x34 can be assumed to be different from the mean value for the general population for Control_36x34, or the difference is statistically significant. Effect size: d = 0.60 => moderate effect size, indicating that the difference between the mean values of the differences and the expected mean value of the differences is moderate.

Control_46x44 & 3D_CBCT_46x44

Table 5

P-value	0.002614
T	-3.2562
Sample size(n)	34
Average of differenceces ($\overline{x_d}$)	-0.2397

SD of differences (S_d)	0.4293

From the above data, with the established p-value (0.00) < α => H0 is rejected in favor of H1. This means that the mean value for the general population for 3D_CBCT_46x44 can be assumed to be different from the mean value for the general population for Control_46x44, or the difference is statistically significant. Effect size: d = 0.56 => moderate effect size, indicating that the difference between the mean values of the differences and the expected mean value of the differences is moderate.

Control_34x31/41 & 3D_CBCT_34x31/41

Table 6

P-value	0.001068
T	-3.5506
Sample size(n)	38
Average of differenceces ($\overline{x_d}$)	-0.2076
SD of differences (S_d)	0.3605

From the above data, with the established p-value (0.00) < α => H0 is rejected in favor of H1. This means that the mean value for the general population for 3D_CBCT_34x31/41 can be assumed to be different from the mean value for the general population for Control_34x31/41, or the difference is statistically significant. Effect size: d = 0.58 => moderate effect size, indicating that the difference between the mean values of the differences and the expected mean value of the differences is moderate.

Control_44x31/41 & 3D_CBCT_44x31/41

Table 7

P-value	1.85e-8
T	-7.1393
Sample size(n)	38
Average of differenceces ($\overline{x_d}$)	-0.44
SD of differences (S_d)	0.3799

From the given data, with the established p-value (0.00) < α => H0 is rejected in favor of H1. This means that the mean value for the general population for 3D_CBCT_44x31/41 can be assumed to be different from the mean value for the general population for Control_44x31/41, or the difference is statistically significant. Effect size: d = 1.16 => large effect size, indicating that the difference between the mean values of the differences and the expected mean value of the differences is large.

Methods for task 2

1. Placement of composite markers.
2. Physical measurements.
3. Intraoral scanning.
4. Conducting measurements on digital models from intraoral scanning.

Methods 1 and 2 from Task 2 coincide with methods 1 and 2 from Task 1.

INTRAORAL SCANNING

Preparing the intraoral scanner for scanning:

Before scanning with 3Shape Trios (Copenhagen, Denmark), we start the scanning software and place the camera on the workstation. Upon opening the software, we select "New patient" and enter the patient's initials. Then, under "Add case instructions," we enter "Research." Next, we choose "Scan only" and click "Next," initiating the camera's warming-up process before use. After it's warmed up, we attach the scanning mirror (Fig. 19) to it (Fig. 20) and proceed with its calibration. For this, a special Color Calibration Target (Fig. 21) is used, connected to the scanning mirror with an adapter (Fig. 22). The target is positioned with the color scale (marked as "A") pointing upwards towards the adapter, following the manufacturer's instructions for proper calibration. Subsequently, color calibration is performed. After completing the color calibration, we place the target with the gray scale (marked as "B") pointing upwards and calibrate it as well. Once the calibration is finished, we proceed to scanning.

Scanning:

Scanning was performed after saliva extraction using aspiration from the dental unit and drying with an air stream, following the scanning strategy and manufacturer's recommendations (Fig. 23), to reduce the likelihood of digital model deformations. Patients were scanned while avoiding excessive mouth opening during the process. After scanning, a thorough inspection of the obtained model was conducted, checking for incompletely scanned areas as well as deformations or folds in the scan. In the presence of such areas, rescanning of the missed portions was performed, or an entirely new scan was conducted if necessary. If no defects or deformations were detected in the obtained model, it was exported and saved as an .STL file for necessary measurements using appropriate software. The exported files were stored in a folder titled "Intraoral scanners.

Fig. 19. Scanning mirror

Fig. 20. Scanning Mirror Attached to the Scanning Tip

Fig. 21. Calibration Target for 3Shape Trios Intraoral Scanner

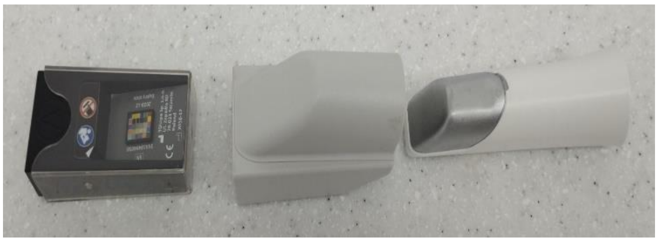

Fig. 22. Calibration Target, Port, Mirror for Intraoral Scanning.

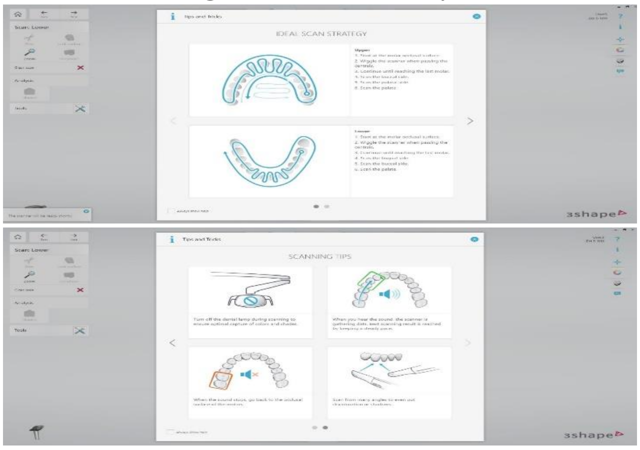

Fig. 23. Scanning Strategy and Manufacturer Recommendations for Intraoral Scanning.

PERFORMING MEASUREMENTS ON DIGITAL DIAGNOSTIC MODELS FROM INTRAORAL SCANNING

To conduct measurements from intraoral scanning, the 3Shape 3DViewer software was used. After launching the software, an empty window is opened, from which we select the dropdown menu "File→Open." Then, we choose a file from the folder "Intraoral scanners" and open it to perform the necessary measurements. The same approach as in measurements on 3D generated models from CBCT was followed to optimize and achieve maximum accuracy in measuring the distances between teeth 36-46, 34-44, 36-34, 46-44, 34 - midline between 31 and 41, 44 - midline between 31 and 41:

1. Placement of a digital marker on the midline between 31 and 41. (Fig. 24)
2. Placement of a digital marker above the composite marker on the buccal surface of 34. (Fig. 25)
3. Placement of a digital marker above the composite marker on the buccal surface of 36 and placing a second one on the first marker on the buccal surface of 34, aiming for maximum alignment of the markers. (Fig. 26)
4. Placement of a digital marker above the composite marker on the buccal surface of tooth 44 and placing a third one on the first and second markers on the buccal surface of tooth 34, striving for maximum alignment. (Fig. 27)
5. Moving the first marker from the buccal surface of tooth 34 onto the marker on the buccal surface of tooth 44. (Fig. 28)
6. Moving the second marker from the buccal surface of tooth 34 onto the buccal surface of tooth 46 above the composite marker. (Fig. 29)

7. Moving a marker from the midline between 31 and 41 onto the marker on the buccal surface of tooth 46, ensuring maximum alignment between the markers. (Fig. 30)

In this way, the distances are measured in the following order:

1. 34 - midline between 31 and 41.
2. 34-36
3. 34-44
4. 44 - midline between 31 and 41.
5. 36-46
6. 44-46

For each intraoral scan, the measurements are conducted in this order to reduce the possibility of placing the markers in different positions each time. All measurements were made on a computer with the following specifications: Processor Intel(R) Core(TM) i7-9700F CPU @ 3.00GHz 3.00 GHz; RAM 16.0 GB, 64-bit operating system running Windows 10 Pro. The workstation is equipped with 2 18-inch monitors. (Fig. 18)

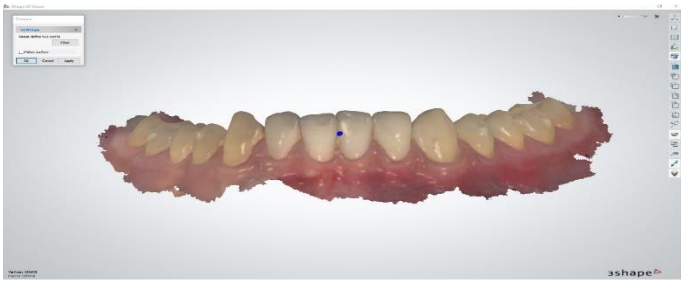

Fig. 24

Fig. 25

Fig. 26

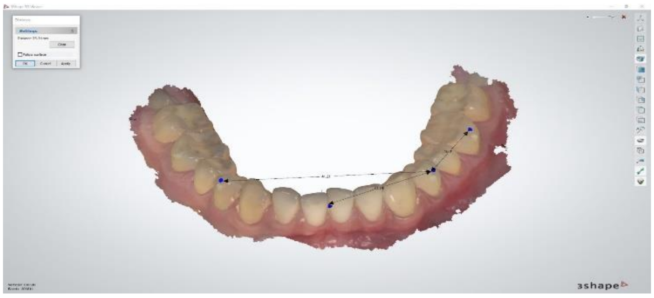

Fig. 27

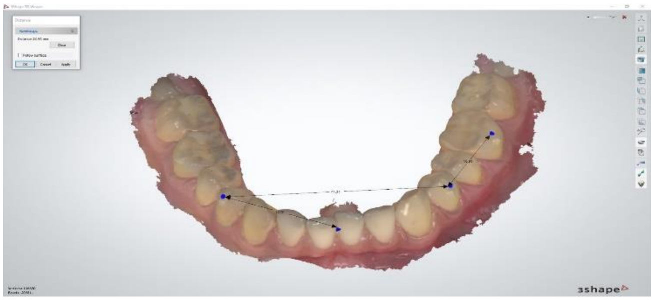

Fig. 28

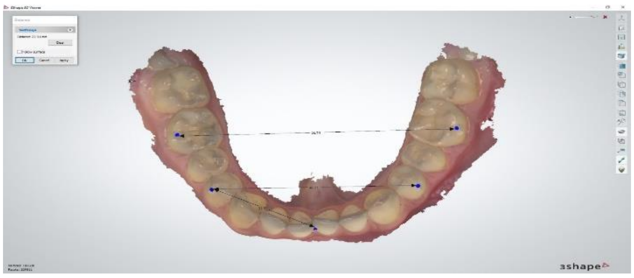

Fig. 29

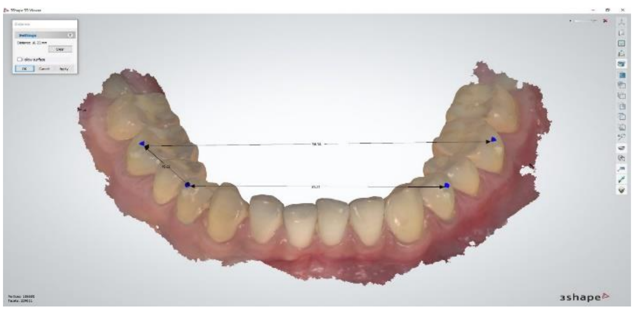

Fig. 30

Results for task 2

Table 8 presents descriptive characteristics of the measurements made on the 3D reconstruction from the intraoral scanner.

Table 8

Linear measurments	Modalities	N	Mean	SD	SE	CI 95% for Mean		Min	Max
						Low	Up		
46x36, mm	Physical measurments	36	48.893	3.33	0.56	47.77	50.02	41.06	56.60
	IOS	36	48.960	3.40	0.57	47.81	50.11	40.52	56.61
44x34, mm	Physical measurments	38	36.59	2.80	0.45	35.67	37.51	30.53	41.53
	IOS	38	36.45	2.88	0.47	35.51	37.40	29.75	41.39
36x34, mm	Physical measurments	37	15.84	1.07	0.18	15.49	16.20	13.70	18.20
	IOS	37	16.02	1.01	0.17	15.68	16.35	14.33	17.99
46x44, mm	Physical measurments	36	15.41	2.29	0.38	14.63	16.18	8.47	20.39
	IOS	36	15.64	2.46	0.41	14.81	16.47	8.15	20.94
34x31/41, mm	Physical measurments	38	20.49	1.53	0.25	19.99	20.99	16.84	23.62
	IOS	38	20.73	1.59	0.26	20.21	21.25	17.58	24.12
44x31/41, mm	Physical measurments	38	20.69	1.57	0.26	20.17	21.21	17.35	24.16
	IOS	38	21.04	1.56	0.25	20.53	21.56	18.06	24.52

Analysis for task 2

Comparing the results from linear measurements of interdental distances in the lower jaw between direct intraoral measurements with a digital caliper and those made on generated diagnostic models from an intraoral scanner (3Shape Trios) led to the following observations:

Control_46x36 & IOS_3Shape_46x36

Table 9

P-value	0.2542
T	-1.1611
Sample size(n)	33
Average of differenceces ($\overline{x_d}$)	-0.06939
SD of differences (S_d)	0.3433

From the aforementioned data, with the established p-value (0.25) > α => H0 cannot be rejected. This means that the average value for the general population for IOS_3Shape_46x36 can be assumed to be equal to the average value for the general population for Control_46x36. Effect size: d = 0.20 => a small effect size, indicating that the difference between the average values of the differences and the expected average values of the differences is small.

Control_44x34 & IOS_3Shape_44x34

Table 10

P-value	0.06259
T	1.92
Sample size(n)	38
Average of differenceces ($\overline{x_d}$)	0.1361
SD of differences (S_d)	0.4368

From the aforementioned data, with the established p-value (0.06) > α => H0 cannot be rejected. This means that the average value for the general population for IOS_3Shape_44x34 can be assumed to be equal to the average value for the general population for Control_44x34. Effect size: d = 0.31 => a small effect size, indicating that the difference between the average values of the differences and the expected average values of the differences is small.

Control_36x34 & IOS_3Shape_36x34

Table 11

P-value	0.06214
T	-1.9269
Sample size(n)	36
Average of differenceces ($\overline{x_d}$)	-0.1664
SD of differences (S_d)	0.5181

From the provided data, with the established p-value (0.06) > α => H0 cannot be rejected. This means that the average value for the general population for IOS_3Shape_36x34 can be assumed to be equal to the average value for the general population for Control_36x34. Effect size: d = 0.32 => a small effect size, indicating that the difference between the average values of the differences and the expected average values of the differences is small.

Control_46x44 & IOS_3Shape_46x44

Table 12

P-value	0.0152
T	-2.561
Sample size(n)	34
Average of differenceces ($\overline{x_d}$)	-0.2441
SD of differences (S_d)	0.5558

From the given data, with the established p-value (0.02) < α => H0 is rejected in favor of H1. This means that the average value for the general population for IOS_3Shape_46x44 can be assumed to be different from the average value for the general population for Control_46x44, or the difference is statistically significant. Effect size: d = 0.44 => a small effect size, indicating that the difference between the average values of the differences and the expected average values of the differences is small.

Control_34x31/41 & IOS_3Shape_34x31/41

Table 13

P-value	0.0009002
T	-3.6107
Sample size(n)	38
Average of differenceces ($\overline{x_d}$)	-0.2434
SD of differences (S_d)	0.4156

From the given data, with the established p-value (0.00) < α => H0 is rejected in favor of H1. This means that the average value for the general population for IOS_3Shape_34x31/41 can be assumed to be different from the average value for the general population for Control_34x31/41, or the difference is statistically significant. Effect size: d = 0.59 => a medium effect size, indicating that the difference between the average values of the differences and the expected average values of the differences is moderate.

Control_44x31/41 & IOS_3Shape_44x31/41

Table 14

P-value	0.000004334
T	-5.3804
Sample size(n)	38
Average of differenceces ($\overline{x_d}$)	-0.3558
SD of differences (S_d)	0.4076

From the given data, with the established p-value (0.00) < α => H0 is rejected in favor of H1. This means that the average value for the general population for IOS_3Shape_44x31/41 can be assumed to be different from the average value for the general population for Control_44x31/41, or the difference is statistically significant. Effect size: d = 0.87 => a large effect size, indicating that the difference between the average values of the differences and the expected average values of the differences is substantial.

Methods for task 3:

1. Placement of composite markers.
2. Physical measurements.
3. Taking a conventional impression: a) with A-silicone, b) with polyether.
4. Removal of composite markers.
5. Casting of plaster models.
6. Measurements on plaster models.

Methods 1 and 2 for Task 3 coincide with methods 1 and 2 for Task 1.

TAKING CONVENTIONAL IMPRESSIONS:

- **TAKING AN IMPRESSION WITH A-SILICONE**

Initially, impressions were taken with A-silicone for each participant in the study due to the risk of inhibition of the polymerization reaction of this type of impression material when the prosthetic field is contaminated with residues of polyethers. We started by selecting an appropriate tray size based on the size of the lower jaw for each participant in the study. We used metal perforated trays from Medesy (Italy) due to the high density of the putty material from A-silicone to avoid tissue compression during impression taking (Fig. 31). Each tray was coated with Universal Tray Adhesive (Zhermarck) (Fig. 32) left to dry for 10 minutes before taking the impression. We used a one-step two-phase technique with A-silicone Elite HD+ Putty Soft Normal set (Zhermarck) in combination with Elite HD+ Light body Normal set (Zhermarck) (Fig. 33).

Fig. 31. Metal Perforated Impression Tray from Medesy (Italy)

Fig. 32. Zhermack Tray Adhesive.

Fig. 33. Tray adhesive (Zhermack), Elite HD+ Putty Soft Normal set (Zhermack), and Elite HD+ Light body Normal set (Zhermack).

For the Elite HD+ Putty Soft, we mixed equal amounts of base and catalyst measured using measuring spoons (different ones for the two masses). Mixing was done within 45-60 seconds following the manufacturer's recommendations. We used latex-free gloves to reduce the risk of inhibition of the silicone polymerization process. After mixing, the material was applied to the selected tray. The Light body material was mixed using a silicone gun and mixing tips in a 1:1 ratio. It was applied on top of the putty material before placing the tray in the patient's mouth. According to the manufacturer's recommendations, the setting time in the patient's mouth was 3:30 minutes. To ensure complete polymerization, we extended the waiting time by a minute and a half, totaling 5 minutes. After the impression material had fully set, we removed the tray from the patient's mouth, rinsed it under running water, sprayed it with a disinfectant, and placed it in a bag labeled with the patient's initials.

- **TAKING IMPRESSIONS WITH POLYETHER**

Again, we first selected an appropriate tray size according to the patient's lower jaw size. We used standard metal "Rim Lock" trays (Fig. 34) with preapplied Polyether Adhesive (3M ESPE) (Fig. 35), which was applied 10 minutes before taking the impression and left to dry thoroughly. We used "closed" trays to prevent the polyether material from flowing out due to its lower viscosity compared to the putty-like consistency of silicone we used

Fig. 34. Standard metal tray type "Rim Lock"

Fig. 35. Polyether Adhesive (3M ESPE)

The polyether impression material we used is Impregum Monophase (3M ESPE) (Fig. 36), which is mixed using the Pentamix 3 (3M ESPE) automatic mixing machine (Fig. 37). Before loading it into the tray, it's necessary to allow some of the mixed material to flow out until a consistent color is achieved.

Fig. 36. Impregum Monophase 3M ESPE

Fig. 37. Pentamix 3 (3M ESPE)

The setting time in the mouth is 3 minutes and 15 seconds. To ensure complete polymerization of the material, we extended this time by a minute and a half, making it a total of 4:45 minutes. After the impression material was set, we removed the tray from the patient's mouth, rinsed it with running water, sprayed it with disinfectant, and placed it in a pouch labeled with the patient's initials. The two impressions (Fig. 38) were stored in separate pouches.

Fig. 38. Impressions (left - Elite HD+ Putty Soft Normal set (Zhermack) and Elite HD + Light body Normal set (Zhermarck); right - Impregum Monophase (3M ESPE))

REMOVAL OF COMPOSITE MARKERS

After conducting physical measurements, cone-beam computed tomography, and capturing digital and conventional impressions, we removed the composite markers placed on the vestibular surfaces of lower first molars and first premolars. For this purpose, we used a white Arkansas stone with a flame-shaped tip for a contra-angle handpiece (KaVo) running at 10,000 rotations per minute with water cooling.

POURING OF GYPSUM MODELS

The gypsum models were poured within 12 hours after taking the conventional impressions. We used dental gypsum class 4 Fujirock EP Premium Line Pastel Yellow (Fig. 39). The water-to-gypsum ratio was maintained according to the manufacturer's recommendations. Mixing was performed using a vacuum mixer Renfert Twister venturi (Fig. 40) for one minute at a speed of 450 rpm, reaching 100% vacuum. Then, the gypsum was poured into the impressions placed on a vibrating table Vibrax 230V/50Hz Renfert (Fig. 41) set at intensity level 3 and low-frequency working mode until achieving maximum gypsum flow into the impression. Afterward, the gypsum was poured into the rubber mold for models, and the impression tray with the impression material was placed on the mold.

Fig. 40

Fig. 41

Fig. 41. Vibrating Table Vibrax 230V/50Hz Renfert

The setting time for this gypsum is between 9-12 minutes, but the models are removed from the impressions 24 hours after pouring (Fig. 42).

Fig. 42. Ready Plaster Models

MEASUREMENTS ON PLASTER MODELS

After the plaster models have set, we have two models from each volunteer in the study – one from the impression with A-silicone (Elite HD+ Putty Soft Normal set (Zhermarck) + Elite HD + Light body Normal set (Zhermarck)) and one from the impression with polyether (Impregum Soft, 3M ESPE). Upon releasing the models, measurements were conducted using a digital caliper, Kinex (Kinex measuring, Czech Republic), with a range of 0-300 mm, jaw length of 60 mm, and a resolution of 0.01 mm. We measured linear distances on the lower jaw between teeth 36-46, 34-44, 36-34, 46-44, 34 - midline between 31 and 41, 44 – midline between 31 and 41, following the sequence of intraoral measurements (Fig. 43).

Fig. 43. Sequence of Measurements with Digital Caliper.

The measurements were recorded in millimeters with a precision of a tenth of a millimeter. The protrusions on the models on the buccal surface of the first molars and first premolars of the lower jaw obtained during the impression with composite buttons served as a reference when conducting the measurements – the jaws of the caliper were placed over the buttons as close as possible to them when measuring the distances between teeth 36-46, 34-44, 36-34, 46-44. When measuring the distances between 34 - midline between 31 and 41 and 44 - midline 31 and 41, one end of the jaws was placed on a point between the central recession in the middle third of the respective teeth. Before each new measurement, the caliper was zeroed and calibrated to reduce the likelihood of errors in the measurements. The measured values will be recorded in a table in Word 2019 (Microsoft) format (Appendix 1), which will later be transferred to Excel 2019 (Microsoft).

Results for task 3

Table 15 presents descriptive characteristics of the measurements made on reconstructions of the dentition through plaster models from elastomeric impression materials (Impregum Monophase and Elite HD+).

Table 15

Linear measurments	Modalities	N	Mean	SD	SE	CI 95% for Mean		Min	Max
						Low	Up		
46x36, mm	Physical measurments	36	48.893	3.33	0.56	47.77	50.02	41.06	56.60
	Impregum gypsum models	36	48.889	3.31	0.55	47.77	50.01	41.21	56.90
	Elite HD+ gypsum models	36	48.849	3.37	0.56	47.71	49.99	41.44	56.84
44x34, mm	Physical measurments	38	36.59	2.80	0.45	35.67	37.51	30.53	41.53
	Impregum gypsum models	38	36.72	2.91	0.47	35.76	37.68	29.96	41.76
	Elite HD+ gypsum models	38	36.65	2.90	0.47	35.70	37.61	29.78	41.74
36x34, mm	Physical measurments	37	15.84	1.07	0.18	15.49	16.20	13.70	18.20
	Impregum gypsum models	37	15.94	0.98	0.16	15.61	16.26	13.85	17.87
	Elite HD+ gypsum models	37	15.95	1.06	0.17	15.60	16.31	13.85	18.19
46x44, mm	Physical measurments	36	15.41	2.29	0.38	14.63	16.18	8.47	20.39
	Impregum gypsum models	36	15.42	2.34	0.39	14.62	16.21	8.49	20.72
	Elite HD+ gypsum models	36	15.41	2.34	0.39	14.62	16.20	8.50	20.19
34x31/41, mm	Physical measurments	38	20.49	1.53	0.25	19.99	20.99	16.84	23.62
	Impregum gypsum models	38	20.48	1.61	0.26	19.95	21.01	16.60	24.70
	Elite HD+ gypsum models	38	20.49	1.64	0.27	19.95	21.03	16.52	24.31
44x31/41, mm	Physical measurments	38	20.69	1.57	0.26	20.17	21.21	17.35	24.16
	Impregum gypsum models	38	20.71	1.63	0.26	20.17	21.24	17.81	24.50
	Elite HD+ gypsum models	38	20.75	1.64	0.27	20.21	21.29	17.96	24.56

Analysis for Task 3

Comparing the results of linear measurements of interdental distances in the lower jaw between direct intraoral measurements with a digital caliper and those made on diagnostic plaster models using Impregum Monophase led to the following observations:

Control_46x36 & Impregum_46x36

Table 16

P-value	0.6893
T	-0.4034
Sample size(n)	33
Average of differenceces ($\overline{x_d}$)	-0.03364
SD of differences (S_d)	0.479

From the above data, with the established p-value (0.69) > α, H0 cannot be rejected. This means that the average value for the general population for Impregum_46x36 can be considered equal to the average value for the general population for Control_46x36. Effect size: d = 0.07 => very small effect size, indicating that the difference between the average values of the differences and the expected average values of the differences is very small.

Control_44x34 & Impregum_44x34

Table 17

P-value	0.09975
T	-1.6884
Sample size(n)	38
Average of differenceces ($\overline{x_d}$)	-0.1342
SD of differences (S_d)	0.49

From the above data, with the established p-value (0.10) > α, H0 cannot be rejected. This means that the average value for the general population for Impregum_44x34 can be considered equal to the average value for the general population for Control_44x34. Effect size: d = 0.27 => small effect size, indicating that the difference between the average values of the differences and the expected average values of the differences is small.

Control_36x34 & Impregum_36x34

Table 18

P-value	0.2132
T	-1.2678
Sample size(n)	36
Average of differenceces ($\overline{x_d}$)	-0.08694
SD of differences (S_d)	0.4115

From the above data, with the established p-value (0.21) > α, H0 cannot be rejected. This means that the average value for the general population for Impregum_36x34 can be considered equal to the average value for the general population for Control_36x34. Effect size: d = 0.21 => small effect size, indicating that the difference between the average values of the differences and the expected average values of the differences is small.

Control_46x44 & Impregum_46x44

Table 19

P-value	0.4048
T	-0.844
Sample size(n)	34
Average of differenceces ($\overline{x_d}$)	-0.05912
SD of differences (S_d)	0.4084

From the provided data, with the established p-value (0.40) > α, H0 cannot be rejected. This means that the average value for the general population for Impregum_46x44 can be considered equal to the average value for the general population for Control_46x44. Effect size: d = 0.14 => very small effect size, indicating that the difference between the average values of the differences and the expected average values of the differences is very small.

Control_34x31/41 & Impregum_34x31/41

Table 20

P-value	0.8536
T	0.1858
Sample size(n)	38
Average of differenceces ($\overline{x_d}$)	0.01184
SD of differences (S_d)	0.393

From the provided data, with the established p-value (0.85) > α, H0 cannot be rejected. This means that the average value for the general population for Impregum_34x31/41 can be considered equal to the average value for the general population for Control_34x31/41. Effect size: d = 0.03 => very small effect size, indicating that the difference between the average values of the differences and the expected average values of the differences is very small.

Control_44x31/41 & Impregum_44x31/41

Table 21

P-value	0.7441
T	-0.3288
Sample size(n)	38
Average of differenceces ($\overline{x_d}$)	-0.02079
SD of differences (S_d)	0.3897

From the provided data, with the established p-value (0.74) > α, H0 cannot be rejected. This means that the average value for the general population for Impregum_44x31/41 can be considered equal to the average value for the general population for Control_44x31/41. Effect size: d = 0.05 => very small effect size, indicating that the difference between the average values of the differences and the expected average values of the differences is very small.

Comparing the results of linear measurements of interdental distances on the lower jaw between direct intraoral measurements with a digital caliper and those made on diagnostic gypsum models made from Impregum Monophase led to the following observations:

Control_46x36 & Elite HD_46x36

Table 22

P-value	0.6446
T	0.4657
Sample size(n)	33
Average of differenceces ($\overline{x_d}$)	0.03697
SD of differences (S_d)	0.4561

From the provided data, with the established p-value (0.64) > α, H0 cannot be rejected. This means that the average value for the general population for Elite HD_46x36 can be considered equal to the average value for the general population for Control_46x36. Effect size: d = 0.08 => very small effect size, indicating that the difference between the average values of the differences and the expected average values of the differences is very small.

Control_44x34 & Elite HD_44x34

Table 23

P-value	0.4345
T	-0.7901
Sample size(n)	38
Average of differenceces ($\overline{x_d}$)	-0.06447
SD of differences (S_d)	0.5031

From the provided data, with the established p-value (0.43) > α, H0 cannot be rejected. This means that the average value for the general population for Elite HD_44x34 can be considered equal to the average value for the general population for Control_44x34. Effect size: d = 0.13 => very small effect size, indicating that the difference between the average values of the differences and the expected average values of the differences is very small.

Control_36x34 & Elite HD_36x34

Table 24

P-value	0.1366
T	-1.5236
Sample size(n)	36
Average of differenceces ($\overline{x_d}$)	-0.09972
SD of differences (S_d)	0.3927

From the provided data, with the established p-value (0.14) > α, H0 cannot be rejected. This means that the average value for the general population for Elite HD_36x34 can be considered equal to the average value for the general population for Control_36x34. Effect size: d = 0.25 => small effect size, indicating that the difference between the average values of the differences and the expected average values of the differences is small.

Control_46x44 & Elite HD_46x44

Table 25

P-value	0.3489
T	-0.9502
Sample size(n)	34
Average of differenceces ($\overline{x_d}$)	-0.06353
SD of differences (S_d)	0.3898

From the provided data, with the established p-value (0.35) > α, H0 cannot be rejected. This means that the average value for the general population for Elite HD_46x44 can be considered equal to the average value for the general population for Control_46x44. Effect size: d = 0.16 => very small effect size, indicating that the difference between the average values of the differences and the expected average values of the differences is very small.

Control_34x31/41 & Elite HD_34x31/41

Table 26

P-value	0.9856
T	0.01821

Sample size(n)	38
Average of differenceces ($\overline{x_d}$)	0.001053
SD of differences (S_d)	0.3564

From the provided data, with the established p-value (0.99) > α, H0 cannot be rejected. This means that the average value for the general population for Elite HD_34x31/41 can be considered equal to the average value for the general population for Control_34x31/41. Effect size: d ≈ 0.00 => very, very small effect size, indicating that the difference between the average values of the differences and the expected average values of the differences is very, very small, approaching zero.

Control_44x31/41 & Elite HD_44x31/41

Table 27

P-value	0.2985
T	-1.0545
Sample size(n)	38
Average of differenceces ($\overline{x_d}$)	-0.06368
SD of differences (S_d)	0.3723

From the provided data, with the established p-value (0.30) > α, H0 cannot be rejected. This means that the average value for the general population for Elite HD_44x31/41 can be considered equal to the average value for the general population for Control_44x31/41. Effect size: d = 0.17 => very small effect size, indicating that the difference between the average values of the differences and the expected average values of the differences is very small.

Methods for Task 4

To assess the reliability of measurements, we conducted repeat measurements on 21 3D reconstructions from CBCT, 21 intraoral scan reconstructions, and 42 plaster models (21 made of A-silicone and 21 made of polyether) 2.5 months after the initial measurements. These selections included patients without missing first molars and without existing prosthetic restorations. The measurements were performed using the same software (3D Viewer(3Shape)) and the same caliper as in the initial measurements.

Results for Task 4

The results of the researcher's measurement accuracy for the investigated modalities mostly indicate overestimation of measured lengths during repeat measurements (499 out of 504 cases). Table 28 presents the average difference between repeat measurements. Only 2 out of all measurements showed statistically significant differences (P < 0.005).

Table 28

IOS	N	**Mean dif (M1-M2), мм**	**SD**	**SE**	**Lower limit CI 95%**	**Upper limit CI 95%**	**p**
46x36, мм	21	-0.221	0.360	0.072	-0.385	-0.058	0.01*
44x34, мм	21	-0.167	0.454	0.115	-0.374	0.040	0.107
36x34, мм	21	-0.086	0.257	0.152	-0.203	0.031	0.140
34x31/41, мм	21	-0.067	0.429	0.115	-0.263	0.128	0.482
44x31/41, мм	21	-0.073	0.325	0.132	-0.221	0.074	0.313
IOS		**Me dif (M1-M2), мм**	**Q1;Q3**	**IQR**	**Тест**		**p**
46x44, мм		-0.0300	-0.275; 0.275	0.55	Wilcoxon test		0.931
3D CBCT	**N**	**Mean dif (M1-M2), мм**	**SD**	**SE**	**Lower limit CI 95%**	**Upper limit CI 95%**	**p**
46x36, мм	21	-0.077	0.683	0.149	-0.388	0.234	0.613
44x34, мм	21	0.040	0.540	0.118	-0.206	0.286	0.738
36x34, мм	21	-0.034	0.574	0.125	-0.295	0.227	0.790
46x44, мм	21	-0.100	0.836	0.183	-0.480	0.281	0.592
34x31/41, мм	21	-0.134	0.435	0.095	-0.332	0.064	0.172
44x31/41, мм	21	0.035	0.338	0.074	-0.119	0.189	0.638
Impregum	**N**	**Mean dif (M1-M2), мм**	**SD**	**SE**	**Lower limit CI 95%**	**Upper limit CI 95%**	**p**
44x34, мм	21	-0.157	0.407	0.089	-0.342	0.029	0.093
36x34, мм	21	0.071	0.604	0.132	-0.203	0.346	0.594
34x31/41, мм	21	-0.003	0.471	0.103	-0.217	0.212	0.978
44x31/41, мм	21	-0.239	0.451	0.098	-0.444	-0.034	0.025*
Impregum	**N**	**Me dif (M1-M2), мм**	**Q1;Q3**	**IQR**	**Тест**		**p**
46x36, мм	21	-0.150	-0.400; 0.180	0.580	Wilcoxon test		0,100
46x44, мм	21	-0.150	-0.415;0.240	0.655	Wilcoxon test		0,258
Elite HD+	**N**	**Mean dif (M1-M2), мм**	**SD**	**SE**	**Lower limit CI 95%**	**Upper limit CI 95%**	**p**
46x36, мм	21	-0.093	0.328	0.072	-0.243	0.056	0.207
44x34, мм	21	-0.113	0.528	0.115	-0.353	0.128	0.339
36x34, мм	21	0.028	0.697	0.152	-0.289	0.345	0.855
46x44, мм	21	-0.022	0.679	0.148	-0.331	0.287	0.881
34x31/41, мм	21	0.016	0.527	0.115	-0.224	0.256	0.889
44x31/41, мм	21	-0.180	0.605	0.132	-0.455	0.096	0.189

Analysis for Task 4

The results of the study on the researcher's measurement reliability for the investigated modalities demonstrate a correlation coefficient ranging from moderate to excellent, with very high statistical significance. These results are presented in Table 29.

Table 29

Linear measurments		IOS		CBCT		Impregum		Elite HD+	
	N	**r**	**p**	**r**	**p**	**r**	**p**	**r**	**p**
46x36, mm	21	0.995**	<0.0001	0.977	<0.0001	0.981**	<0.0001	0.995**	<0.0001
44x34, mm	21	0.989**	<0.0001	0.983	<0.0001	0.991**	<0.0001	0.984**	<0.0001

36x34, mm	21	0.958**	<0.0001	0.803	<0.0001	0.834**	<0.0001	0.740**	<0.0001
46x44, mm	21	0.802**	<0.0001	0.848	<0.0001	0.850**	<0.0001	0.888**	<0.0001
34x31/41, mm	21	0.971**	<0.0001	0.969	<0.0001	0.965**	<0.0001	0.956**	<0.0001
44x31/41, mm	21	0.982**	<0.0001	0.980	<0.0001	0.967**	<0.0001	0.944**	<0.0001

4.DISCUSSION

From the obtained results, it can be concluded that concerning the accuracy of measuring the distance between the first molars of the lower jaw (46x36), all investigated modalities exhibit exceptional precision. For the Impregum group, the lowest average difference value (-0.033±0.479) was observed, indicating a tendency to overestimate. In the Elite HD+ group, the average difference value is close (0.036±0.456) to that of Impregum, but with a reverse tendency to underestimate. The highest average difference value was observed in 3D-generated models from CBCT (-0.128±0.428) with a tendency to overestimate, although this was not statistically significant (p-value – 0.094).

In the intraoral scanners group, there is a tendency to overestimate the measured values except for the distance 34-44, where there is an underestimation for the average difference value (0.136±0.436). In the intraoral scanners group, a statistically significant difference was observed for some of the measured distances – 46x44 (p-value – 0.015), 34x31/41 (p-value – 0.0009), 44x31/41 (p-value – 0.000004). For 46x44, a small effect size was determined (d=0.44), indicating the lack of practical significance for the average difference value (-0.244±0.555). For 34x31/41 and 44x31/41, respectively, a medium (d=0.59) and large (d=0.87) effect size was observed, indicating higher practical significance for the average difference values at 34x31/41 (-0.243±0.415) and 44x31/41 (-0.355±0.407).

The group of elastomeric impression materials (Impregum Monophase and Elite HD+) performed equally well for all conducted linear measurements. In the Impregum group, there was a tendency to overestimate almost all measured values except for 34x31/41 (0.011±0.393), with no statistical significance observed for any of the measured distances. Similarly, in the Elite HD+ group, no statistically significant differences were found in the measurements. For some measured distances, underestimation was observed (46x36 (0.036±0.456); 34x31/41 (0.001±0.356)), while overestimation was noted for the remaining measurements (44x34 (-0.064±0.503); 36x34 (-0.099±0.392); 46x44 (-0.063±0.389); 44x31/41 (-0.063±0.373)).

For some of the measured linear distances, intraoral scanners performed equally well with elastomeric impression materials, while for others, there was a statistically significant difference compared to the controls. Regarding the measurement of the distance between the first premolars and the midline between central incisors, 3Shape Trios performed worse than the tested conventional materials.

In measurements on 3D-generated models from CBCT scans, significant deviations were observed compared to control measurements except for the distance 36-46, where no statistically significant difference was found (p-value – 0.094). This method demonstrated significant differences for all other measurements and was unsatisfactory in terms of accuracy compared to control measurements. Underestimation of measurements was observed only for 44x34 (0.146±0.406), while for all others, there was overestimation – 46x36 (-0.128±0.428); 36x34 (-0.271±0.45); 46x44 (-0.239±0.429); 34x31/41 (-0.207±0.36); 44x31/41 (-0.44±0.379). The effect size was largest for 44x31/41 (d=1.16), while it was moderate for 34x31/41 (d=0.58), 46x44 (d=0.56), and 36x34 (d=0.60). A small effect size was observed for 46x36 (d=0.30) and 44x34 (d=0.36).

Despite establishing practical significance (moderate/large effect size) for some of the obtained values, it does not necessarily imply clinical significance. The majority of measurements were within 1 mm difference compared to the controls, indicating clinical acceptability.

Regarding reliability, all tested modalities proved to be reliable. However, a tendency to overestimate measured lengths was observed during repeated measurements. Currently, there is no literature data found from in-vivo studies conducted in the manner we chose – physical measurements intraorally from the lower jaw, serving as controls. Devan Naidu and colleagues compared the accuracy of intraoral scanners with measurements from a digital caliper, but on gypsum models from previously taken alginate impressions. The challenge in collecting patient data through physical measurements is the inability to replicate measurements at any given time. Organizing a study in this manner requires meticulous planning of the time needed to collect all data and access to various materials and technologies – intraoral scanner, automatic mixing machine for impression material, cone-beam computed tomography machine. The placement of buttons is a factor that can influence subsequent measurements since it is challenging to control their exact positioning and size. This, in turn, can affect measurements with the caliper, as we positioned the jaws on the caliper precisely above the buttons during measurements. Composite buttons are also registered during intraoral scanning, cone-beam computed tomography scanning, and impressions with elastomers, serving the same purpose – as reference points for measurements on the reconstructed lower jaw, which we compared with physical measurements. To minimize the risk of composite buttons detaching (especially when taking a conventional impression), we used etch and bond before placing the composite on the buccal surfaces of the teeth. This ensured no composite button came off during data collection. The technique for placing composite buttons proved reliable, and we recommend it when there's a need to register and transfer reference points from the oral cavity to digital or gypsum models. In our study, each participant was a separate experimental setup. For each participant, physical measurements (made intraorally with a digital caliper with an accuracy of up to 0.1 millimeters) served as controls compared to measurements on reconstructions from the tested modalities. All data were collected by the same operator, which might also influence the measurements. Even the process of using a digital caliper can affect measured values, regardless of its sampling device. Another essential aspect that can influence measurements, especially concerning measurements in the distal areas of the oral cavity, is the degree of mouth opening. Patients who can open wide make it much easier to measure interdental distances between the first molars in the third and fourth quadrants. The most challenging distances to register in all patients were those between the sixth and fourth teeth in the third and fourth quadrants, due to the size of the caliper we used. A caliper with shorter jaws would cause inconvenience when measuring in distal areas. We recommend replacing the battery when using a digital caliper for measurements. Cleaning the caliper, especially the jaws, should be done with the batteries removed to reduce the risk of damage.

In our study, we utilized the same CBCT machine for all participants and applied consistent scanning parameters. Subsequently, the obtained files in .DICOM format were converted using specialized software into .STL format, enabling us to conduct similar linear measurements on the generated 3D reconstructions of the lower jaw.

One of the primary challenges in visualizing images obtained through CBCT scanners is the formation of artifacts, which can stem from various sources. The phenomenon of "beam hardening" causes deformations in the image around areas with highly radiopaque materials (such as metals, zirconium, and composites).

For specific participants in the study (those with zirconium crowns on lower six teeth - two of them on teeth 46 and one on tooth 36), it was impossible to perform linear measurements because the model in these areas exhibited significant deformations. This presents a challenge when placing digital markers in the precise positions necessary for accurately measuring linear distances. Thus, the generated reconstructions are primarily applicable to patients without existing prosthetic restorations (on natural teeth or implants).

An extremely important requirement during cone-beam computed tomography (CBCT) scanning is for the patient to remain as still as possible to avoid the occurrence of "Motion artifacts," which could create imperfections in the scanned image. In this context, participants were positioned vertically with a special cushion under the chin, their heads were stabilized in a fixed position, and their jaws were secured with a plastic bite plate during the scanning process. It is essential to note that the stable position of the head does not directly influence the accuracy of the scanned object, as proven in the literature. However, significant attention was paid to ensuring that all patients were maximally centered during scanning.

According to some researchers, the voxel size does not significantly affect the accuracy and reliability of measurements on 3D models generated through CBCT. In our study, all scans were performed with isotropic voxels sized at 0.150 mm.

During scanning, we separated the patients' jaws using a plastic plate that was bitten down with the cutting edges of the central incisors. This facilitated the visualization of interproximal areas. The volume of the scanning field was set to 10x10 due to medical requirements, necessitating the inclusion of the upper jaw, which was a limiting factor in our study. This could affect the visibility of tooth surfaces and interproximal areas and influence the accuracy of measurements on 3D models. According to Bassan Hassan, there is a significant loss of quality in 3D models with a large scanning field. We cannot confirm this assertion as we did not investigate the influence of this factor.

In the work of Marcelo Lupion Poleti and colleagues, an in vitro study was conducted to assess the reliability and accuracy of linear measurements on 3D models generated from CBCT, using standard predefined thresholds in two software programs for segmentation. The findings from this study indicate that linear measurements on 3D models created using standard predefined thresholds in Dolphin and InVesalius software are considered reliable and accurate when compared to physical measurements. In our study, we used InVesalius version 3.1 software to convert .DICOM files to .STL format, but we cannot determine the specific influence of the software on the generated models. In our study, the models generated using this method stood out as the least accurate compared to those examined, although we did not find this to have clinical significance. InVesalius software is known for its user-friendly interface, as it does not require in-depth knowledge to operate. Learning the steps to convert .DICOM to .STL files does not take much time - about one day. This underscores that working with this software is accessible even to ordinary users, without requiring special computer knowledge or parameters.

Most studies establish high accuracy in the conducted linear measurements on 3D models generated from CBCT. These studies use dry skulls and jaws for their experiments, some of which include simulating soft tissues around the scanned object. However, this kind of experimental design cannot fully replicate the conditions in real patients. J.K. Dusseldorp and colleagues have pointed out that the accuracy of segmenting 3D models from the hard tissues of the craniofacial complex and the lower jaw obtained from CBCT may be affected by the presence of soft tissues, with their influence possibly falling below the generally accepted level of clinical significance, around 1 mm. They also recommend further research in this area since the level of accuracy might not meet the requirements of procedures where high precision is crucial. In our study, we focused on the accuracy of measurements of interdental distances in the lower jaw, where the requirements for precision are not as high. Nevertheless, we found statistically significant differences compared to the controls. This aspect emphasizes the importance of our research approach and contributes to a better understanding of the accuracy of measurements on 3D models, especially in clinical scenarios. Despite the statistically significant differences, our results are also below the generally accepted level of clinical significance, around 1 mm. Our study provides valuable data regarding the reliability of 3D models generated from CBCT scanners using real patients. This represents a significant step forward in understanding the possibilities and limitations of these models in clinical applications. The fact that we used real patients contributes to the realistic reproduction of clinical scenarios and adds complexity to the study. Additionally, our efforts to standardize the measurement process across different models, as well as the use of the same software, contribute to minimizing possible variations and errors associated with different steps of the study.

Danielle R. Periago and colleagues found that most of the linear measurements made in their study significantly differed from anatomical dimensions; however, most of them can be considered sufficiently accurate clinically for craniofacial analysis. This aligns with the results from our study.

In the study conducted by CA Lascala and colleagues, it was found that the measured distances on CBCT files tend to underestimate compared to those made using a digital caliper on dry skulls. Nevertheless, they are reliable for linear measurements to assess structures closely related to dentomaxillofacial imaging. Sebastian Baumgaertel and colleagues observed that dental measurements conducted on 3D reconstructions from CBCT can be used for quantitative analysis as they prove to be highly reliable, although there is a tendency for these measurements to slightly underestimate anatomical truth. In our study, there is a tendency to overestimate the measured distances, but we agree that 3D reconstructions from CBCT are suitable for conducting quantitative analyses.

Mija Kim and colleagues, in addition to measuring accuracy, assessed reliability and found that values from repeated measurements show excellent reliability with a high intraclass correlation coefficient, corresponding to the results of our study. High intraclass correlation coefficients were also identified by Thais Maria Freire Fernandes and colleagues. They found that caution should be exercised in linear measurements on 3D images since the measurements are reliable but not precise, aligning with the results of our study.

The comparative evaluation between models generated from CBCT scanners and those from intraoral scanners provides valuable data on the accuracy and reliability of both approaches. Such a direct comparative assessment further supports our observations and conclusions. Our study will make a positive contribution to the existing literature, complementing it with real clinical data and providing valuable insights into the use of 3D reconstructions from CBCT scanners in orthodontics (for linear measurements). However, our study is based on real patients, creating conditions for potential errors starting from those related to the scanning process, continuing through file conversion and 3D model generation, and ending with measurements using the software we selected.

Intraoral scanners have been studied by numerous research teams and appear to be a reliable alternative to conventional methods for creating non-removable constructions, both on natural teeth and implants. They find applications in the creation of partial and complete removable prosthetic constructions, Digital Smile Design, pins, obturators for defects in the hard palate, as well as in aligner treatments. Intraoral scanners, as part of CAD-CAM technologies, also play a role in pediatric dentistry, including patients with special needs. This technology is increasingly penetrating various fields of dental medicine, but there is still a need for studies to establish its limitations and possibilities.

Every year, new intraoral scanner systems appear on the market, making it challenging to study the accuracy and reliability of each one of them. There are numerous factors that can influence these parameters in different systems: the operating mode, light source, the need for scanning powder before scanning, the operational process, various non-contact optical technologies, the type of final file, and others. Some of these factors are beyond the control of dental practitioners as they are related to the production process and technologies of different scanners. On the other hand, as operators, we can control certain aspects during scanning that may affect the accuracy of the generated models.

One of the most recognizable intraoral scanners is the 3Shape Trios. This system has been the subject of study in some of the conducted research to date, but there are still no studies entirely focused on the performance of a specific scanner under different clinical or laboratory conditions.

Most studies have been conducted under experimental setups, where factors related to working on patients were eliminated – factors such as the possibility of movement during scanning, gag reflex, saliva, presence of cheeks and tongue, and limitations in mouth opening. This certainly has a positive impact on the accuracy of research results.

In our study, we used the Trios 4 intraoral scanner (3 Shape) and scanned only the lower jaw of real patients while placing them in a stable position with a stabilized headrest on the dental chair. This way, we generated a digital diagnostic model on which we performed linear measurements resembling orthodontic analyses. One of our goals was to establish the accuracy of linear measurements made on reconstructions of the lower jaw from an intraoral scanner compared to intraoral measurements with a digital caliper.

In clinical practice, there are numerous factors that can influence the accuracy of the created model. Gan Ning and his team prove that even the width of the dental arch can affect scanning accuracy, but this is an aspect we cannot directly control. The bending of the lower jaw, known as "mandibular flexure," can also affect the accuracy of the model compared to the real clinical situation, but there is no objective way to determine the degree of this bending. For this reason, during scanning, we encouraged patients not to open their lower jaw too wide. Saliva is a factor that can affect the accuracy of the model, so before each scan, we used a three-function spray handle to dry the area of the lower jaw, and then used aspiration from the dental unit to remove saliva as much as possible.

Lighting and temperature are also crucial factors that should not be overlooked when considering their impact on the accuracy of intraoral scanners. Certain studies recommend turning off the light from the dental unit to minimize unwanted effects. The same principles for optimal color capture are supported by 3Shape's recommendations. In the context of our research, we conducted intraoral scans with the unit light turned off and maintained the ambient temperature at levels around 22-24 degrees Celsius.

Scanning strategy is a factor that affects the accuracy of the digital impression and is directly dependent on the operator's actions. According to observations by A. Ender and A. Mehl, available intraoral scanning systems demonstrate high accuracy in generating impressions for the entire dental arch when appropriate scanning strategies are employed. Priscilla Medina-Sotomayar and colleagues studied different scanning strategies for four intraoral scanners and found that this aspect has a stronger influence on the accuracy of scanning for some devices compared to others. Based on the findings of these studies, we decided to follow the scanning strategy for the lower jaw according to the manufacturer's recommendations. Currently, there are intraoral scanners with improved technologies that facilitate the scanning process without strictly requiring adherence to a specific strategy. However, access to these devices remains limited due to their financial implications.

Studies by Peter Rehmann and collaborators emphasize that calibrating intraoral scanners before use has a positive impact on scanning accuracy. For this reason, we performed calibration before each scanning. This process does not require significant time in clinical practice but is usually not done before every patient scan.

According to the results of the study by Ji-Won Anh, tooth alignment was not considered a determining factor in selecting patients for the current dissertation. Patients wearing braces and implants were excluded from the study since the presence of such elements can influence scanning results and would certainly impact the cone-beam computed tomography scanning process.

Based on our observations, regarding comfort and speed, the intraoral scanner used by us performed exceptionally well, consistent with the conclusions of other studies. The average time required for scanning was about 1 minute, which was definitely shorter than the time needed for taking conventional impressions. We did not register any cases where patients experienced a gag reflex. It is worth noting that we scanned only the lower jaw, avoiding proximity to trigger zones such as the back of the palate. An additional advantage of working with 3Shape Trios 4 was the ability to rescan specific areas if the results were not satisfactory, without the need for an entirely new scan. This provided convenience and saved time. Moreover, we had the opportunity to immediately assess the quality of the obtained model in its real colors, which is not possible with conventional impression methods.

Regarding the drawbacks we noticed while working with intraoral scanners, we can highlight the size of the scanning mirror, which somewhat hindered capturing the distal areas of the lower jaw in some of our patients.

To perform linear measurements on the created models, we utilized specialized software (3Shape 3D Viewer). As a guide for placing markers between specific points, we utilized pre-attached composite buttons on the vestibular surfaces of teeth 46, 36, 44, and 34. Ensuring the accuracy of measurements required precise positioning of digital markers. It was crucial to follow a specific sequence when placing the markers and measuring between the points, as this stage carried the potential risk of error. The protocol we employed was tailored to the limitations of the software, allowing us to perform up to three linear measurements simultaneously. This protocol was detailed in section 3.2. The same software and protocol were used for measurements on the 3D models generated through CBCT.

The limitations of measurements conducted this way are directly related to the constraints of the software used. One of the main challenges we encountered was the accurate placement of more than one digital marker on the same point on the surface of the digital model. This could potentially influence the measurements conducted. Working with the software itself required additional time for familiarization.

Under these conditions, the models generated and measurements conducted with intraoral scanners are satisfactory compared to control measurements made using a digital caliper directly in the participants' mouths in this study. Similar conclusions were drawn in Devan Naidu's study, despite differences in the study designs. According to Andreas Ender et al.'s study, digital systems do not significantly differ in capturing the entire dental arch accurately, but high-precision conventional impression materials provide higher accuracy than digital methods, aligning with our study's results. Several studies found that intraoral scanning systems demonstrate similar accuracy to models obtained from polyvinyl siloxane and polyether impression materials for single teeth, and according to others, they are even more precise. Given the limitations of our study, we cannot confirm or refute the claims from these studies. Ala Omar Ali conducted a study comparing the accuracy of digital impressions obtained with different digital impression systems. They found that some of the systems studied show no significant differences compared to scans from conventional impression materials in a three-unit fixed prosthesis scenario. However, other systems provide results with less precision than those from conventional methods. Andres Ender et al., in their clinical study, found that quadrant scanning has a level of accuracy comparable to a model obtained from a conventional impression (polyvinyl siloxane) with a sectorial tray. Conventional impression methods with a rigid full-arch tray demonstrate the highest precision compared to all tested digital systems. There are differences in precision among different digital systems, but all fall within the range where clinically satisfactory restorations can be created. In our study, we tested only one intraoral scanning system, but considering the results, we can confirm what was found by Andres Ender. A. Ender and A. Mehl compared conventional and digital impression methods for the entire dental arch. They reported a similarity in accuracy and precision between polyether impressions and two intraoral scanners. In another study, they concluded that the accuracy and precision of digital impressions (CEREC Bluecam) for the entire arch are less accurate than those of a conventional impression with polyvinyl siloxane, which corresponds to the results of our study. Although the results from intraoral scanner scans are clinically satisfactory, we found higher accuracy in reconstructions from conventional impression materials.

Taking impressions is a routine procedure for dental practitioners, with elastomeric materials being one of the most commonly used types. The primary quality of impression materials is their volumetric stability and accuracy, which depend on the degree of completion of the chemical reaction between the primary components and the type of polymerization reaction. Linear shrinkage in different types of elastomers mainly differs due to the formation of low molecular weight secondary products. According to literature data, the shrinkage after 24 hours varies among different elastomer types, being 0.10% for polyethers and least for addition silicones at 0.05%.

The volumetric stability of impression materials over time can be influenced by several factors: completion of the chemical reaction, formation and evaporation of low molecular weight secondary products (water, alcohol, hydrogen), water sorption (when the material is not hydrophobic), stress relaxation due to specific form and processing methods, and temperature variations between body temperature and room temperature, the impression technique used, the type of impression tray, and factors associated with it.

For the purposes of this study, two impressions were taken from each participant using two different elastomeric impression materials - A-silicone (Elite HD+) and polyether (Impregum Monophase). In the case of A-silicone impressions, a one-phase two-layer technique was used, while for polyether impressions, a one-phase technique was employed. This approach was chosen to optimize the conventional impression process and reduce the possible accumulation of secondary deformations that may occur when using two-step methods, as indicated by some scientific sources. Despite arguments presented for higher accuracy of two-step methods by some authors, other studies do not confirm significant differences between one-step and two-step techniques. Given the results of our study, we believe that the one-phase impression technique using A-silicone and polyether leads to the accurate pouring of gypsum reconstructions of the lower jaw teeth.

For the A-silicone impressions, we used metal perforated trays to reduce the potential risk of deformations during impression taking. This choice was made due to the high density of the paste, which could compress the surrounding tissues during impression taking, as reported in the literature. For polyether impressions, we opted for standard metal trays of the "Rim Lock" type, as Impregum Monophase has lower viscosity, hence reducing the risk of tissue compression. Before taking the impressions, the tray surfaces were treated with an adhesive, left to dry for a minimum period of 10 minutes. According to T.J. Bomberg, this adhesive application phase on the tray represents a critical step in the impression procedure, contributing to more precise and consistent results.

The impressions were taken sequentially, with A-silicone used first, followed by polyether. After accurately dispensing the A-silicone paste and catalyst using the corresponding measuring trays for the base and catalyst, we wore nitrile gloves during their mixing to prevent potential inhibition of the material's polymerization reaction. The dispensing process of the base and catalyst with paste-like materials is prone to potential inaccuracies, regardless of using measuring trays. For the preparation of the corrective material, we used a specialized dispensing gun and a mixing cannula specific to the material. This method ensured optimal mixing of the base and catalyst for the respective material. After successfully homogenizing the paste, the correction material was applied directly onto the already mixed paste. Before placing the tray in the patient's mouth, the prosthetic field was dried, as A-silicones exhibit hydrophobic properties.

Taking impressions with polyether was facilitated in terms of material mixing, as we used Pentamix 3, allowing optimal mixing without creating voids. The material was applied to the tray directly through a single-use mixing cannula. Despite the hydrophilic properties of this material, the prosthetic field was dried before taking the impression. A drawback of using this material was its bitter taste.

The impression-taking procedure with both considered materials took approximately 5 minutes, proving to be more time-consuming compared to the time required for intraoral scanning. In the context of lower jaw impressions, we did not encounter difficulties related to triggering the gag reflex. However, patients preferred the intraoral scanning method for impression-taking. In the case of conventional methods, trying different sizes of impression trays is often necessary before finding the suitable one, requiring subsequent cleaning and autoclaving of the tested trays before they can be reused.

When using analog impressions, there is a risk of deformation after processing with disinfectant. This step is mandatory after removing the impression tray from the patient's mouth and rinsing it with running water, aiming to reduce the probability of infection spreading to the dental laboratory.103 Additionally, if optimal conditions are not maintained during transportation, analog impressions can be subject to deformation.

In comparison, intraoral scanners are characterized by the absence of the risk of cross-contamination since the information transfer occurs digitally. The advantages also include easier communication with the laboratory, as the models can be inspected immediately, whereas in conventional impressions, discrepancies are often identified after the gypsum model has already been cast. The process of casting gypsum models is an additional step in conventional methods, which can lead to the generation of hidden deformations.

A benefit of digital models is that they do not change during our work with them and do not require additional physical space, while gypsum models can break or get damaged during measurements, as well as during transportation, and require storage space.

It would be interesting to 3D print physical models from the available .STL files obtained from intraoral scanning and then conduct measurements using a digital caliper to verify the accuracy of the measurements under these conditions. Alternatively, the gypsum models could be scanned using a laboratory scanner, and measurements could be performed using the same software and protocol that we used for all digital models in this study. Under these conditions, different results might be obtained.

SUMMARY

The dental industry has invested significant efforts in its quest to create a means of obtaining models that closely replicate the intraoral conditions of patients. Conventional impression materials, particularly elastomeric impressions, have proven to be exceptionally reliable over the years, both for generating diagnostic models and for creating prosthetic constructions, although most data regarding these materials are more than a decade old. With the advent of new technologies, especially intraoral scanners, an alternative method for creating models has emerged, shifting the focus of researchers toward these innovations. Intraoral scanners have been on the market for over 40 years and have evolved considerably from the first systems to the ones available today. However, there is still a need for studies regarding their accuracy and reliability in various clinical situations, despite the promising results and advantages they offer in our practice. Technological progress often outpaces the accumulation of information on issues directly impacting dental practitioners because new intraoral scanning systems emerge every year, making it challenging to conduct research on each of them. By the completion of our studies, during which we utilized 3 Shape Trios 4, the 3 Shape Trios 5 was already available. Considering the differences in the design of various scanners as well as their optical systems, it is challenging to assume that they all operate identically. Nevertheless, there is a trend in the dental field toward entirely digital treatment approaches. This necessitates the need for research to enrich our understanding of the capabilities and limitations of intraoral scanners, which accompany the process of digitizing various stages of dental work.

Cone-beam computed tomography (CBCT) is perhaps the most innovative invention in dental imaging diagnostics. Besides conducting comprehensive radiographic analyses, this modality allows us to generate 3D models. Data on the application, advantages, and limitations of models generated using this method are still extremely limited and require further research to gather sufficient information before they become a routine method in dental practice.

In summary, conventional methods and materials still surpass intraoral scanners in terms of the accuracy of the reconstructed models. 3D models generated from CBCT typically exhibit deviations within clinically acceptable values (under 1 mm). While impression materials and intraoral scanners do not pose a direct risk to patients' health and tend to be more accurate in the

generated models, CBCT involves radiation exposure and requires additional processing of the acquired files before they can be used and analyzed.

Regarding accuracy, we can summarize the results as follows:

- Most accurate method: Elite HD+
- Second most accurate method: Impregum
- Less accurate method: 3Shape Trios
- Least accurate method: 3D model generated from CBCT study

Given the limitations of this study, we believe there is a need for additional research to gather more data on this topic. Conventional methods and modern technologies do not exclude each other but rather complement one another. We should strive to leverage the best of both worlds based on specific clinical situations.

CONCLUSIONS:

1. All investigated modalities demonstrate high reliability.
2. Linear measurements on gypsum reconstructions of the lower jaw obtained from elastomer impressions provide the highest measurement accuracy compared to controls.
3. Gypsum reconstructions obtained from silicone impressions demonstrate higher accuracy than those obtained through polyether impressions.
4. 3D reconstructions from CBCT (New Tom Giano HR) with a FOV of 10x10 exhibit the lowest accuracy in linear measurements among the investigated modalities.
5. The application of 3D reconstructions generated from CBCT (New Tom Giano HR) scans is impractical in the presence of highly radiopaque materials in the scanning area.
6. Measurements on reconstructions from intraoral scanning (3Shape Trios 4) are more accurate than those on 3D reconstructions from CBCT (New Tom Giano HR).
7. Measurements on reconstructions from intraoral scanning (3Shape Trios 4) tend to overestimate compared to control intraoral measurements with a digital caliper.
8. Measurements on 3D reconstructions generated from CBCT (New Tom Giano HR) tend to overestimate compared to control intraoral measurements with a digital caliper.
9. Measurements on gypsum models from Impregum Monophase tend to overestimate compared to control intraoral measurements with a digital caliper.
10. Measurements on gypsum models from Elite HD show no specific tendency for overestimation or underestimation compared to control intraoral measurements with a digital caliper.
11. The single-phase two-layer technique with Elite HD is a reliable method for generating gypsum reconstructions of the lower jaw.
12. The single-layer technique with Impregum Monophase is a reliable method for generating gypsum reconstructions of the lower jaw.

13. Converting .DICOM to .STL files using InVesalius 3.1 software is a quick and convenient method.

14. 3D Viewer (3 Shape) proved to be a reliable software for conducting linear measurements.

15. Considering the ALARA principle, assigning CBCT for the purpose of generating 3D reconstructions is not justified given their current limitations.

16. Separating the jaws during CBCT scanning facilitates the segmentation process when generating 3D reconstructions.

CONTRIBUTIONS:

Contributions with confirmatory character:

1. It was confirmed that elastomeric impression materials are more accurate than intraoral scanners for generating dental occlusion reconstructions.
2. It was confirmed that A-silicones are more accurate than polyethers for generating gypsum dental occlusion reconstructions.
3. The reliability of all tested modalities was confirmed.
4. It was confirmed that it is impossible to generate 3D reconstructions from CBCT for diagnostic purposes (conducting measurements) in the presence of radiopaque materials in the scanning area.
5. It was confirmed that the generated 3D models are not as accurate with a large scanning field of view (FOV).
6. The advantage of separating the two jaws during scanning with cone-beam computed tomography for the subsequent segmentation process was confirmed.

Contributions with an original character for the country:

1. For the first time in Bulgaria, an in-vivo study was conducted, generating 3D dental occlusion reconstructions of the lower jaw after scanning with cone-beam computed tomography.
2. For the first time in Bulgaria, the accuracy of 3D dental occlusion reconstructions of the lower jaw obtained from cone-beam computed tomography scans was compared with those from intraoral scanning, A-silicone impressions, and polyether impressions.

Publications related to the dissertation work

1. Kostadinov, K., Peev, S., Hristov, I., "Accuracy of intraoral scanners and factors influencing it" – International Journal of Medical Dentistry

2. Kostadinov, K., Peev, S., Hristov, I., "3D models generated by CBCT and their application in dentistry" – International Journal of Medical Dentistry

3. Kostadinov, K., Peev, S. "|Accuracy and reliability of lower dental arch reconstructions"| - Scripta Scientifica Medicinae Dentalis